Re-examination of safety parameters using kinetic theory of nano-granular flows

Jacques Bouillard, Philippe Marchal, François Henry, Alexis Vignes, Olivier Dufaud, Laurent Perrin, Edouard Plasari

Journal of Physics: Conference Series **304** (2011) 012079 doi:10.1088/1742-6596/304/1/012079

Re-examination of safety parameters using kinetic theory of nano-granular flows

Jacques Xavier Bouillard[1], Philippe Marchal[2], François Henry[1], Alexis Vignes[1], Olivier Dufaud[2], Laurent Perrin[2] and Edouard Plasari[2]

[1]INERIS, Parc ALATA, 60550 Verneuil en Halatte, France

[2]ENSIC, 1 rue Grandville, LRGP-UPR-CNRS-3349, 54000Nancy, France

Abstract. The origin of the kinetic theory of granular flow was originally credited to Bagnold [1]. By using a very primitive expression of the particle collision frequency, he derived an expression for the repulsive pressure of the particles in uniform shear flows. His repulsive pressure was proportional to the square of the velocity gradient and the particle diameter and directly proportional to the particle density. This theory was later extended by Savage [2] and Gidaspow [3]. Such theories provide insight on the dependence of the viscosity, and various moduli (elastic, non elastic, viscous…) in terms of the granular temperature and the associated shear-rates. Until recently, such parameters were difficult to measure because of the lack of specifically designed equipment. This challenge was successfully taken up and resolved by P. Marchal of ENSIC who designed a new rheometer for powders (figure 1). This equipment can put in evidence the importance of the granular temperature on the elastic and viscous behaviors of the granular flows. Such rheological behavior is important in risk analysis for nanopowders, because as the nanopowder may be subjected to process shear rates and stresses, its structural and topological changes, in terms of the transformation of agglomerates into primary nanoparticles, have strong impacts on emission factors of nanosized particles that can be released in the environment or into a workplace from such dense-phase nanopowder processes. Such transformation can be analyzed by studying the nano-granular rheological signature of the system. Such risk assessment approach using these new fundamental rheological safety parameters is described in this paper.

1. Introduction

The use of the concept of granular temperature for dense and dilute suspended powder has evolved since the 80s in theories and applications aiming at explaining turbulence, rheology and reactivity in such systems. The heart of the approach consists in expressing the granular temperature, θ, defined as follows [3,4]:

$$3\,\theta = (c_x^2 + c_y^2 + c_z^2)$$

where *c* is the particle fluctuating velocity, as described below.

This approach is based on the development of kinetic theory for gas–solids two-phase flow based on the theory for non-uniform dense gases described in Chapman and Cowling [5] and the pioneering paper of Lun *et al.* [4] in applying the kinetic theory of gases to granular flows. The kinetic theory approach uses one equation model to determine the turbulent kinetic energy (or granular temperature) of the particles and assumes either a Maxwellian distribution for the particles, or a non-Maxwellian distribution for both dilute and dense cases. The kinetic theory approach for granular flow allows the determination of the pressure and viscosity of the solids in place of empirical relations [6]. One of the

major goals in the use of such theory was the evaluation from first principles of the viscosity of granular media.

Various kinetic theory approaches considering the effect of the interaction of particle and gas phase, and particle collisions have been applied to the study of a gas–solids flow in risers of circulating fluidized beds, chutes and dense phase mixing [7-9]. Extensions of these approached have included the modeling of agglomeration via the effects of Van der Waals forces [10]. Such approaches were successful in reproducing two-phase flow experiments performed by Miller and Gidaspow [11].

2. Gas–solids flow model description

The model adopted is based on the fundamental concept of interpenetrating continua for multiphase mixtures. According to this theory different phases can be present at the same time in the same computational volume. Such an idea is made possible by the introduction of a new dependent variable, the concentration, ε_i of each phase *i*. The fundamental equations of mass, momentum, and energy conservation are then solved for each considered phase. Appropriate constitutive equations have to be specified in order to describe the physical rheological properties of each phase and to close the conservation equations. In this model, solids viscosity and pressure are derived by considering the random fluctuation of particle velocity and its variations due to particle–particle collisions and the actual flow field. Such a random kinetic energy, or granular temperature, can be predicted by solving, in addition to the mass and momentum equations, a fluctuating kinetic energy equation for the particles. The solids viscosity and pressure can then be computed as a function of granular temperature at any time and position. Particles are considered smooth, spherical, inelastic, and undergoing binary collisions. The adoption of the second approximation distribution function allows us to apply the theory to both dense and dilute two-phase flows. A more complete discussion of the implemented kinetic theory model can be found in Gidaspow [3].

The basic Hydrodynamic equations governing granular flows are given below [3]:

- Continuity equation for phase k: $\frac{\partial(\rho_k \varepsilon_k)}{\partial t} + \nabla.(\rho_k \varepsilon_k v_k) = \dot{m}_k$

- Momentum equation for phase k: $\frac{\partial(\rho_k \varepsilon_k v_k)}{\partial t} + \nabla.(\rho_k \varepsilon_k v_k v_k) = \varepsilon_k \rho_k \tilde{g} + \nabla.[\tau_k] + \sum_l^N \beta(v_l - v_k) + \dot{m}_k \widetilde{v_k}$

  acceleration of phase "k" = buoyancy + stress + drag force + phase change

- Constitutive equation for stress (above min. fluidization): $[\tau_k] = \left[-P_k + \xi_k \nabla v_k\right][I] + 2\mu_k[S_k]$

  $$[S_k] = \frac{1}{2}[\nabla v_k + (\nabla v_k)^T] - \frac{1}{3}\nabla. v_k[I]$$

and the granular temperature governing equations [3]:

- Fluctuating energy equation: $\frac{3}{2}\left[\frac{\partial}{\partial t}\left(\varepsilon_s \rho_s \theta\right) + \nabla.\left(\varepsilon_s \rho_s v_s \theta\right)\right] = \bar{\bar{\tau}}_s : \nabla v_s - q - \gamma_s + \beta_A \langle C_g . C_p \rangle - 3\beta_A \theta$

  Collisional energy dissipation: $\gamma_s = 3(1-e^2)\varepsilon_s^2 \rho_s g_o \theta \left(\frac{4}{d_s}\sqrt{\frac{\theta}{\pi}} - \nabla. v_s\right)$

  Conductivity of fluctuating energy: $\kappa = \frac{2}{(1+e)g_o}\left[1 + \frac{6}{5}(1+e)g_o \varepsilon_s\right]^2 \kappa_{dil} + 2\varepsilon_s^2 \rho_s d_s g_o (1+e)\sqrt{\frac{\theta}{\pi}}$

  Dilute phase (Eddy type) granular conductivity: $\kappa_{dil} = \frac{75}{384}\sqrt{\pi \rho_s} d_s \theta^{1/2}$

- Gas-solid drag coefficients [3]:
  - Based on Ergun equation, for $\varepsilon_g < 0.8$: $\beta = 150\frac{\varepsilon_s^2\mu_g}{\varepsilon_g(d_p\phi_s)^2} + 1.75\frac{\rho_g\varepsilon_s|v_g - v_s|}{d_p\phi_s}$

  - Based on single sphere drag, for $\varepsilon_g > 0.8$: $\beta = \frac{3}{4}C_d\frac{\rho_g\varepsilon_s\varepsilon_g|v_g - v_s|}{d_p\phi_s}\varepsilon_g^{-2.65}$

$$C_d = \frac{24}{Re_p}\left[1 + 0.15Re_p^{0.687}\right] \quad for\ Re_p < 1000$$

$$C_d = 0.44 \quad for\ Re_p > 1000$$

where

$$Re_p = \frac{\varepsilon_g\rho_g d_p|v_g - v_s|}{\mu_g}\varepsilon_g^{-2.65}$$

From these equations the viscosity and rheological stresses (Solids pressure and viscosities) can be modeled as follows [3]:

- Solid phase stress:
  - Solid-phase pressure: $P_s = \rho_s\varepsilon_s\theta[1 + 2(1+e)g_o\varepsilon_s]$

  - Solid-phase bulk viscosity: $\lambda_s = \frac{4}{3}\varepsilon_s^2\rho_s d_s g_o(1+e)\sqrt{\frac{\theta}{\pi}}$

  - Solid-phase shear viscosity: $\mu_s = \frac{2\mu_{s_{dil}}}{(1+e)g_o}\left[1 + \frac{4}{5}(1+e)g_o\varepsilon_s\right] + \frac{4}{5}\varepsilon_s^2\rho_s d_s g_o(1+e)\sqrt{\frac{\theta}{\pi}}$

  - Radial distribution function [1] $g_o = \left[1 - \left(\frac{\varepsilon_s}{\varepsilon_{s,max}}\right)^{1/3}\right]^{-1}$

  - Solid-phase dilute viscosity $\mu_{s_{dil}} = \frac{5\sqrt{\pi}}{96}\rho_p d_p\theta^{1/2}$

These equations can be extended for mixtures of powders of different size as shown in Table 1 (see Gidaspow [3]).

To make it simple, in a vibrated shear flow, the total reorganization frequency λ^{-1} can simply be expressed as the sum of the frequencies corresponding to a process of vibration and a process of shear, so one can express the frequency as:

$$\lambda^{-1} = \frac{\dot{\gamma}}{\gamma_c} + \boldsymbol{f} \qquad \textit{Equation (1)}$$

In other words, λ is the mean life time of intergranular contacts, when the sample is submitted to shear and vibrations. Hence, the granular system can be viewed as a temporary elastic network and the magnitude of impulse per grain *i*, transmitted from a fast-moving layer, in the *x* direction, to a slower adjacent one.

On can express the steady state viscosity as:

$$\eta = \frac{\sigma}{\gamma_c f + \dot{\gamma}} \qquad \textit{Equation (2)}$$

Thus, the model predicts a non-Newtonian rheological behaviour for dense-phase vibrated powders, bounded by two extreme flow regimes:

- at high shear rates , the viscosity varies as an inverse function of the shear rate,
- at low frequencies, *f*, the stress becomes independent of the shear rate (Newtonian regime).

Another way of looking at this expression is to start from the general case of the solids phase shear viscosity definition, and take the limit as ε_s becomes relatively large (that is we consider a dense phase), at a constant energy ($\varepsilon_s\theta_s$ = ct). The resulting viscosity is dependant of $\varepsilon_s\theta_s^{1/2}$ or $\theta_s^{-1/2}$ or f^{-1}, hence indicating an inverse function of the viscosity with respect to the shear rate or frequency. Note that the beauty of the modeling approach described earlier is that it provides analytical expressions of the rheological property dependency with respect to the particle diameter, its density and restitution coefficient. This is indeed these dependencies that are exploited to measure the agglomeration energy of nanoparticles via rheological routes.

Table 1. Constitutive relations for a mixture of M phases with rotation [3].

Granular temperature definition	$3m_i\theta_i = \frac{1}{2}m_i\langle c_i^2\rangle + \frac{1}{2}I_i\langle\omega_i^2\rangle$
Number of binary collisions per unit volume, *Nij*	$N_{ij} = 2\sqrt{2\pi}d_{ij}^2 n_i n_j \sqrt{\overline{\theta_{ij}}}\left[1 - 3\overline{\Delta_{ij}} + \cdots\right]$ where $\overline{\Delta_{ij}^2} = \frac{(w_i\theta_i - w_j\theta_j)^2}{(\theta_i+\theta_j)(w_i^2\theta_i + w_j^2\theta_j)}$ and the mean oscillating viscosity $= \left(\overline{\theta_{ij}}\right)^{\frac{1}{2}}$ is expressed in terms of *i* and *j* granular temperatures, θi and θj and the previous groups shown below: $\overline{\theta_{ij}^{\frac{1}{2}}} = \left(\frac{1}{2\theta_i\theta_j A_{ij}}\right)^{\frac{3}{2}} \frac{1}{\left(2D_{ij}\right)^2}$ $= \left(\frac{m_{ij}^2\theta_i\theta_j}{(\theta_i+\theta_j)(m_i^2\theta_i + m_j^2\theta_j)}\right)^{\frac{3}{2}} \left(\frac{m_{ij}^2\theta_i\theta_j}{m_i^2\theta_i + m_j^2\theta_j}\right)^{\frac{1}{2}}$ with the coefficients *Aij*, *Bij* and *Dij* originally obtained by Eirik Manger (1996) as follows $A_{ij} = \frac{1}{2}\left(\frac{1}{\theta_i} + \frac{1}{\theta_j}\right)$, $B_{ij} = \frac{1}{2m_{ij}}\left(\frac{m_i}{\theta_j} - \frac{m_j}{\theta_i}\right)$, and $D_{ij} = \frac{1}{2m_{ij}^2}\left(\frac{m_i^2}{\theta_j} - \frac{m_j^2}{\theta_i}\right)$
Viscosity coefficients and collisional pressure [3]	Collisional viscosity for phase *i*: $\mu_{c,i} = \sum_{k=1}^{M}\mu_{c,ij}$ $\mu_{c,ij} = \frac{3}{2\pi}(1+e)\frac{d_{ij}^4}{d_{pj}^3 d_{pj}^3} g_{ij}\varepsilon_i\varepsilon_j\left(1 + 6\Delta_{ij}^2 + \cdots\right)\overline{\theta_{ij}^{\frac{1}{2}}}$ Solid Viscosity for Dilute Flow: $\mu_{i,kinetic} = \frac{5}{16d_i^2}\left(\frac{m_i^2}{\pi}\theta_i\right)^{1/2}$
Mixture viscosity, μ_m (from sum of phase momentum balances)	$\varepsilon_{sm}\mu_m = \sum_{i=1}^{M}\varepsilon_i\mu_{i,kinetic} + \sum_{i=1}^{M}\varepsilon_i\sum_{j=1}^{M}\mu_{c,ij}$ where ε_{sm} is the sum of the volume fractions of the solids phases.

Equation of state for mixture of M phases	$$Solid\ Pressure = P_s = \sum_{i=1}^{M} \varepsilon_i \rho_i \theta_i + \sum_{i=1}^{M}\sum_{j=1}^{M} P_{c,ij}$$ where the collisional pressure component is: $$P_{c,ij} = \left(\frac{\overline{\theta_{ij}}^{\frac{1}{2}}}{D_{ij}^{\frac{1}{2}}}\right)\frac{\sqrt{2}\pi}{6}(1+e)d_{ij}^3 g_{ij}\frac{\varepsilon_i\varepsilon_j\rho_i\rho_j}{\frac{\pi}{6}\left(\rho_i d_{pi}^3 + \rho_j d_{pj}^3\right)}\left(1 - 3\overline{\Delta_{IJ}} + \cdots\right)$$
Collisional conductivity of phase *i*	$$k_{i,coll} = \frac{1}{2}\sqrt{\frac{\pi}{2}} m_i g_{ij} d_{ij}^4 n_i n_j \left(\frac{\overline{\theta_{IJ}}^{\frac{1}{2}}}{D_{ij}}\right)\left[\frac{8+3\pi}{16\theta_i}S_1 + \frac{m_j}{3m_{ij}\theta_i^2}S_3\right]$$ where $S_1 = \left[1 + \frac{9\pi B^2}{2A_{ij}D_{ij}} + \cdots\right]$ *and* $S_3 = \frac{1}{A_{ij}}\left[1 + \frac{15\pi B^2}{2A_{ij}D_{ij}} + \cdots\right]$ Kinetic conductivity of phase *i:* $k_{i,kinetic} = \frac{15}{4}\mu_i$ $k_i = k_{i,coll} + k_{i,kinetic}$
Energy dissipation, γ_{ij}	$$\gamma_{ij} = \frac{m_i m_j(\theta_i+\theta_j)N_{ij}}{2(m_i+m_j)} \times \left\{\left[\frac{k_i k_j e_t(e_t-1)}{k_i w_i + k_j w_j}\right]\sqrt{\frac{k_j\theta_i + k_i\theta_j}{k_i k_j(\theta_i+\theta_j)}} + \frac{(k_i k_j + k_i w_i + k_j w_j)e_t^2}{4(k_i w_i + k_j w_j)} + \frac{(k_i w_i + k_j w_j - k_i k_j)e_t}{2(k_i w_i + k_j w_j)} + \frac{k_i k_j - 3k_i w_i - 3k_j w_j}{4(k_i w_i + k_j w_j)} + e^2 - 1 + \left[\frac{k_i k_j(e_t^2-1)}{k_i w_i + k_j w_j}\right]\frac{3(k_j\theta_i + k_i\theta_j)}{2k_i k_j(\theta_i+\theta_j)}\right\}$$

3. Description of the rheological viscometer

Considering the macroscopic nature of granular media, we have developed a powder rheometer prototype aiming at compensating for the lack of thermal Brownian motion [12]. It is constituted of a stress-imposed rheometer (AR2000, TA Instruments) (Fig. 1) equipped with a vibration exciter, which is the source of granular temperature. It is connected to an amplifier and controlled through a function generator and an accelerometer connected to a measuring amplifier and fixed to the characterization cell. Attached to the exciter, the characterization cell includes a four blades vane device (radius = R_i = 10 mm; length = L = 30 mm) installed into a cylindrical baffled cup (cup radius = R_c = 25 mm; baffles width = W_b = 5 mm). Such a configuration prevents the powder sample from slipping at the wall and at the surface of the measuring tool as it is equivalent to a tangential annular flow between two vertical coaxial cylinders constituted of the sample itself: the inner cylinder (radius = R_i = 10 mm) is constituted by the part of the sample dragged by the vane blades and the outer cylinder (radius = R_e = R_c - W_b = 20 mm) is constituted by the part of the sample entrapped between the baffles. Considering the geometrical dimensions of the cell, the space between vane and baffle extremities corresponds to a R_e - R_i = 10 mm effective gap, the distance between the base of the vane and the bottom of the cup has been adjusted to the same value.

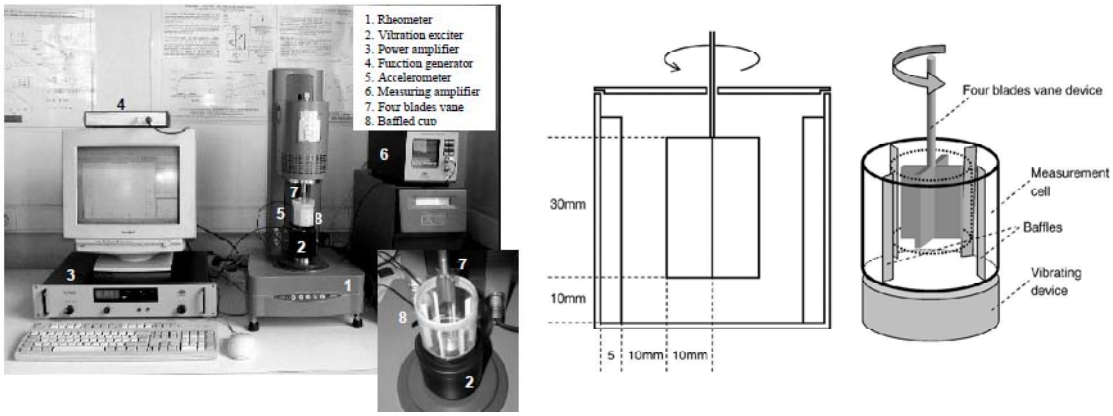

Figure 1. Powder rheometer setup (left), with its schematic representation (right)

With such apparatus, one can readily show the shear thinning rheological behaviors of the powders as shown in Figures 2 and 3, exhibiting an inverse dependency of the viscosity with respect to shear rates at high shear rates.

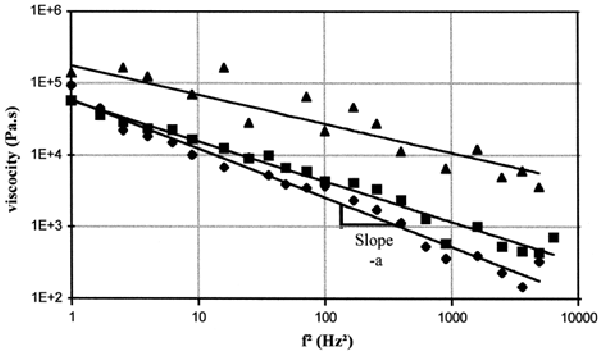

Figure 2. Reduction of viscosity with respect to the granular temperature or equivalently (f^2), for three particle sizes

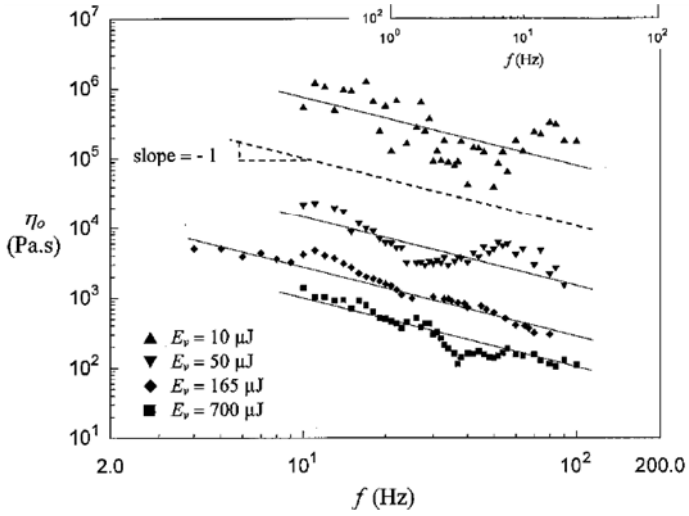

Figure 3. The inverse dependency of the viscosity with respect to the frequency

Over a whole spectrum of shear rates, typical viscosity signatures as shown below can be obtained for various vibration frequencies.

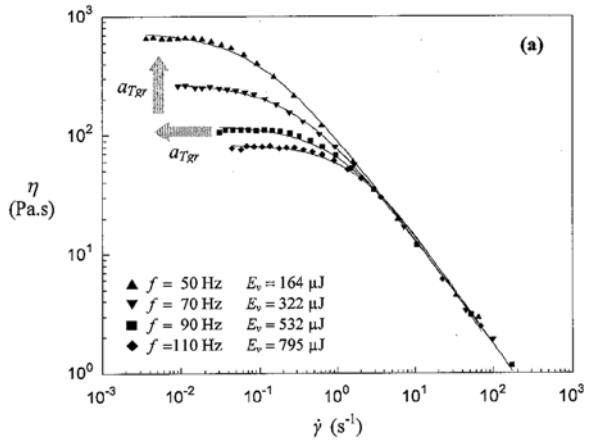

Figure 4. Typical viscosity with respect of shear rate at various vibrating frequencies (granular temperatures), showing the two regimes of Eq *(1)* and *(2)* for a given particle size.

4. Application of Nanopowder Rheological Characteristics for its Use in Risk Evaluation

As shown earlier on, the rheological behavior of a nanopowder depends mainly on four important parameters, the vibration frequency, the shear rate, the particle size and its density (see models above). Hence, if one were to use an agglomerated nanopowder and to test it with the rheometer, on would start measuring the viscosity for a powder equivalent made of large particle sizes. As the shear energy increases, the rheological signatures of the agglomerated nanopowder could significantly exhibit a change in viscous behavior trends as shown in the hypothetical continuous line below. Such change would induce a change of energy supplied by shear that can basically be approximately considered as the agglomeration energy of the powder. Such energy can directly be measured by such device.

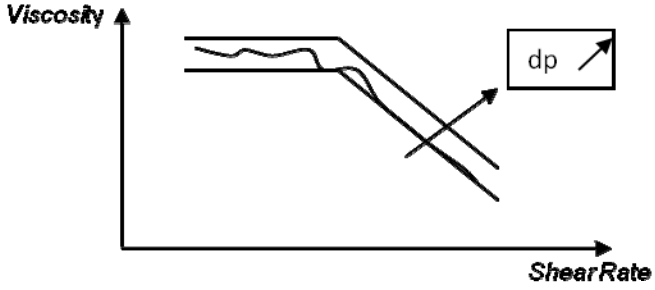

Figure 5. Typical change of the rheological signatures of two powders of different sizes of the same material. In continuous line, the possible outcome of a nanopowder that would be submitted to desagglomeration during its shearing

Two types of Al nanopowders of 120 and 200 nm were studied to evaluate the effect of their mean particle sizes. Particle size distributions of these two nanopowders are represented in Figure 7, in terms of distribution based on the numbers and on the volumes. Of course, a distribution in volume would give advantage to larger particles since they have a larger volume, while the distribution in numbers tends to privilege primary (or smaller) particles. Particle size distributions in number of Al nanopowders are presented in Table 2 which would seem to indicate that despite uncertainties, there is a low degree of agglomeration.

Table 2. Particle size distribution of Al nanopowders

	Particle sizes (μm)		
	d_{10}	d_{50}	d_{90}
Aluminum 100 nm	0,10	0,17	0,62
Aluminum 200 nm	0,15	0,28	0,77

Some clichés made by TEM of these two nanopowders are presented in Figure 6 below:

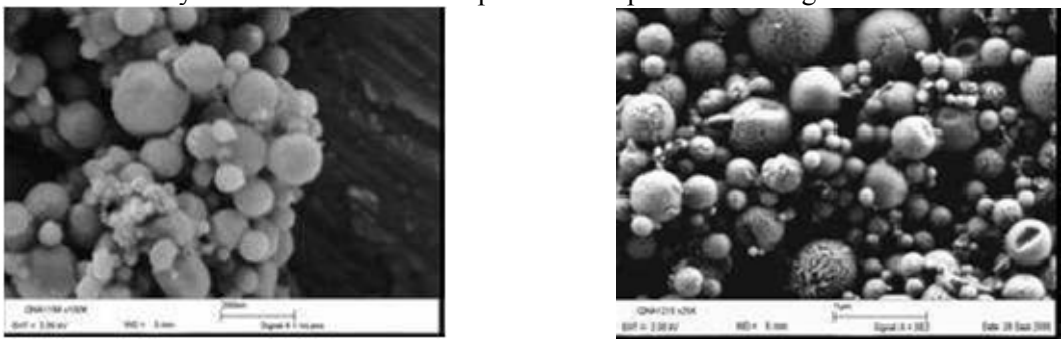

Figure 6. Typical TEM pictures of 120 nm and 200 nm Al particles.

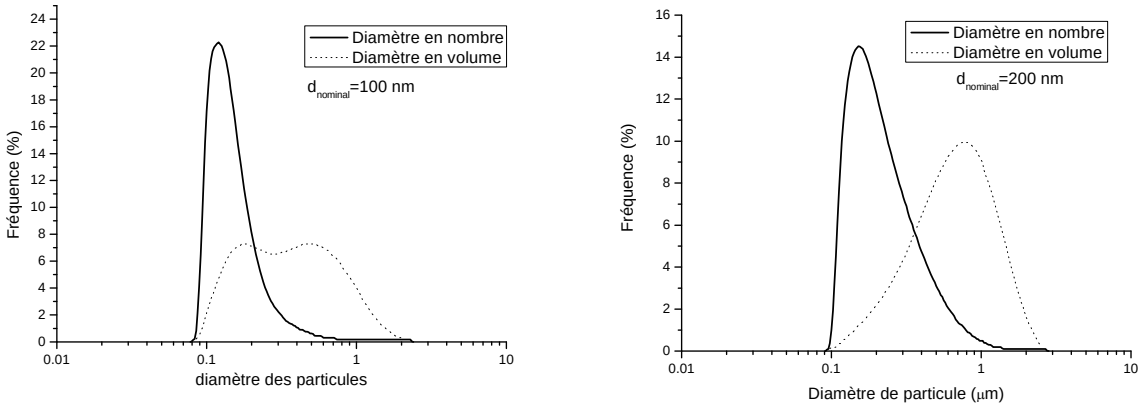

Figure 7. Particle size distribution for 120 nm and 200 nm Aluminum particle sizes.

From rheological measurements made on the two types of powders (120 and 200 nm Aluminum particles as shown in Figure 8), we can see that the two rheological signatures almost follow a same trend at high shear rates. As can also be seen, the rheological signatures differ at low shear rates. This would tend to indicate that at a moderately high shear rates, the powders behave similarly, thus indicating a low degree of agglomeration at such shear rates. This results comfort low degrees of agglomeration observed by particle size distribution measurements as shown in Figure 7. Hence the agglomeration energy is likely to be small, albeit not specifically measured in this study. This would indicate also, a high propensity for this type of powders to be released as primary particles at high shear rates and not as agglomerate particles, inducing therefore potentially higher toxicological risks.

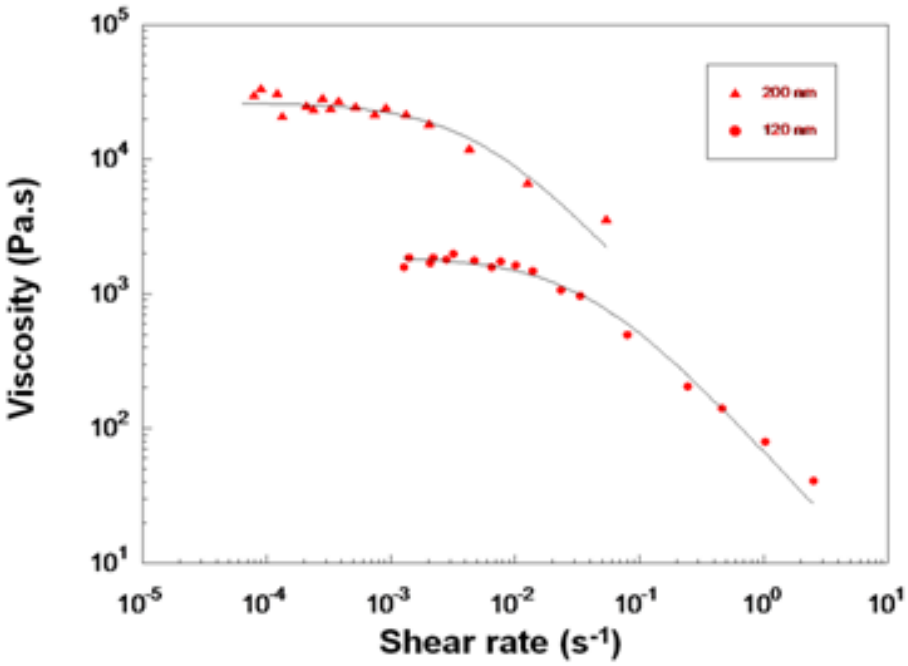

Figure 8. Typical rheological data for 200 nm and 120 nm Aluminum nanoparticles (under a 50Hz base frequency)

This agglomeration energy is therefore a critical safety parameter to consider for the assessment of nanodispersion risks and potential hazards for workers and the environment at large. To evaluate the production rate of primary nanoparticles, one could write the rate of production, r, as

$$r = \alpha \frac{Power\ supplied}{\Delta H_{agglomeration}}$$

where the power supplied is, in the case of the rheometer, the torque power, and the agglomeration energy is the one that can be measured by the technique presented above. As can be seen from this equation, a higher rate of emission of nanoparticles is obtained for powders of low agglomeration energies.

The agglomeration energy, dependent of the type of powder considered under given mechanical constraints, is a measure of the ability of an agglomerated nanopowder to liberate itself into primary nanoparticles at ambient conditions. Hence, this approach could be used for any systems in which a mechanical energy is supplied to a nanopowder, and from which a resulting emission rate is to be evaluated. Once such emission rate is established, then a classical air nanodispersion modeling, integrating reagglomeration mechanisms, can be carried out to evaluate the fate of the released nanoparticles and their potential resulting hazards /risks.

5. Conclusions

Risks induced by the emission of agglomerated particles in a process will essentially depend upon their propensity to release nanoparticles in their primary form, which will strongly depend on the agglomeration energy of the nanopowders. INERIS and LRGP (Nancy) have devised a methodology to first measure the agglomeration energy from rheological characteristics of the nanopowder, by the use of a novel dry phase nanopowder rheometer, and then use this information to evaluate potential risks due to the fate of the potential release in air into more potent primary nanoparticles. Such approach will help nanosafety engineers to evaluate the potential release of nanoparticles from a process using agglomerated nanopowders constrained to mechanical shear stresses. Such new techniques are being the object of the development of new instruments that presently remain confidential.

Nomenclature

Cd	drag coefficient
dp	particle diameter
D_{qs}	rate of energy dissipation
E	restitution coefficient of particles (= 0.999)
g	gravity
$g_{0:}$	radial distribution function
$k_{s:}$	effective thermal conductivity of particles
k_g	thermal conductivity of gas phase
P_g	pressure
P_s	particle pressure
Q	fluctuating energy flux
Re	Reynolds number
T	time
v_g	gas velocity
v_s	particle velocity
u_g	gas velocity
τ_g	gas stress tensor
τ_s	stress tensor of particulate phase
ξ	bulk viscosity
$\theta:$	granular temperature
μ_g	gas viscosity
μ_s	particulate viscosity
ε_g	voidage
ε_s	solid volume fraction
ρ_s	particle density
ρ_g	gas density
β	interphase drag coefficient

References

[1] Bagnold, R. A. (1954). "Experiments on a gravity-free dispersion of large solids spheres in a Newtonian fluid under shear." *Proc. Roy. Soc.* **A225**: 49-63.
[2] Savage, S., B., (1983). Granular Flows at high shear Rates. New York.
[3] Gidaspow, D. (1994). Multiphase Flow and Fluidization: Continuum and Kinetic Theory Descriptions. New York, Academic Press.
[4] Lun, C. K. K. and D. J. J. a. N. C. S.B. Savage (1984). "Kinetic theory for granular flow: inelastic particles in Couette flow and slightly inelastic particles in a general flow field." *J. Fluid Mech.* **140**: 223-235.
[5] Chapman, S. and T. J. Cowling (1961). The Mathematical Theory of Non-Uniform Gases. London, Cambridge University Press.
[6] Campbell, C. S. (2006). "Granular material flows - An overview." *Powder Technology* **162**(3): 208-229.
[7] Huilin, L. and D. Gidaspow (2003). "Hydrodynamics of binary fluidization in a riser: CFD simulation using two granular temperatures." *Chemical Engineering Science* **58**(16): 3777-3792.
[8] Huilin, L., D. Gidaspow, et al. (2002). "Chaotic behavior of local temperature fluctuations in a laboratory-scale circulating fluidized bed." *Powder Technology* **123**(1): 59-68.

[9] Huilin, L., D. Gidaspow, et al. (2003). "Hydrodynamic simulation of gas-solid flow in a riser using kinetic theory of granular flow." Chemical Engineering Journal **95**(1-3): 1-13.
[10] Wang, S., H. Lu, et al. (2007). "Prediction of flow behavior of micro-particles in risers in the presence of van der Waals forces." *Chemical Engineering Journal* **132**(1-3): 137-149.
[11] Gidaspow, M. a. (1992). "Dense, vertical gas–solid flow in a pipe." AIChE **41**: 1801-1813.
[12] Barois-Cazenave, A., P. Marchal, et al. (1999). "Experimental study of powder rheological behaviour." *Powder Technology* **103**(1): 58-64.